Interspeech 2024
1-5 September 2024, Kos, Greece

2.5D Vocal Tract Modeling: Bridging Low-Dimensional Efficiency with 3D Accuracy

Debasish Ray Mohapatra[1], *Victor Zappi*[2], *Sidney Fels*[1]

[1]Department of Electrical and Computer Engineering, University of British Columbia, Canada
[2]College of Arts, Media and Design, Northeastern University, Boston, USA

debasishray@ece.ubc.ca, v.zappi@northeastern.edu, ssfels@ece.ubc.ca

Abstract

We introduce an extended 2D (2.5D) wave solver that blends the computational efficiency of low-dimensional models with the accuracy of 3D approaches tailored for simulating tube geometries similar to vocal tracts. Unlike 1D and 2D models limited to radial symmetry, our lightweight 2.5D finite-difference time-domain solver handles irregular geometries bound only to mid-sagittal symmetry. We validated our model against state-of-the-art 2D and 3D solvers for three different vocal tract geometries, each having a unique cross-sectional shape. Results show that the frequency response of 2.5D simulations closely aligns with 3D up to 12 kHz with a Pearson correlation coefficient greater than 0.8 for all geometries. The proposed model also produces effects of higher-order modes associated with non-cylindrical vocal tracts, surpassing the limitations of the advanced 1D and 2D solvers. Moreover, it achieved a speed-up factor close to an order of magnitude compared to the 2D and 3D models.

Index Terms: vocal tract, articulatory speech synthesis, speech production, FDTD, acoustic simulation

1. Introduction

Modeling sound wave propagation in the upper vocal tract, which connects the larynx to the mouth opening, is challenging due to its complex geometry. The tract's length and cross-sectional shape significantly influence its resonance frequency (i.e., formants). A common approach involves modeling sound propagation within complete three-dimensional (3D) acoustic tubes resembling human vocal tracts. This method employs the numerical solution of 3D linear wave equations [1, 2, 3], incorporating airflow interactions via boundary conditions. The 3D model can approximate the spatiotemporal acoustic pressure variations in the longitudinal and transverse directions. Consequently, it can precisely simulate the effects of perceptually significant higher-order modes—the appearance of resonances and antiresonances in transfer function curves—that vary according to the vocal tract geometries [4]. A major challenge with this methodology is its substantial computational demand. In contrast, one-dimensional (1D) [5] and two-dimensional (2D) [6, 7, 8] models can operate in real-time and yield results akin to 3D models in specific scenarios. These models are well-suited for simulating wave propagation in vocal tract geometries exhibiting only radial symmetry. Nonetheless, numerous situations exist where such geometrical simplifications are infeasible [9, 10], rendering the precise but resource-intensive 3D approach as the sole viable option for the vocal tract acoustic modeling. Moreover, these low-dimensional models can not describe the emergence of transverse modes due to their limited geometrical flexibility [7, 11].

In this paper, we present an extended 2D (2.5D) propagation model that preserves the computational advantages of reduced dimensionality while enabling the numerical simulation of wave propagation in a wide variety of vocal tract geometries. The model utilizes a lightweight 2.5D finite-difference time-domain (FDTD) solver designed to simulate pressure propagation in 3D vocal tracts with the sole constraint of being symmetric in one dimension. Consequently, the 2.5D simulation domain represents 3D tubes with irregular 2D contours (defined along the x and y axes) paired with a depth map that extends along the z axis, symmetrically aligned to the x/y plane. The *depth* component, which represents the extension of a tube along the z axis, can be altered to represent static vocal tracts of unique cross-sectional shapes. As discussed in the next section, the proposed wave solver additionally integrates the mechanical impedance of the vocal tract surface, which vibrates in response to changes in the enclosed pressure. Due to these enhancements, the 2.5D model surpasses the limitations of 1D models, which can only simulate straight cylindrical vocal tracts, and 2D models, which can handle both straight and bent cylindrical vocal tracts. Similar to the 2D model [6], the proposed wave solver is designed for straightforward acceleration on parallel computing devices, like graphics processors, to support real-time speech synthesis applications. A comparative analysis of 2D, 2.5D, and 3D frequency responses for three vowels has been presented. We have evaluated the acoustic characteristics of three distinct tube geometries generated from the area functions of each vowel to underscore the capabilities of the proposed model. These geometries can be characterized by uniform 1D area functions but unique cross-sectional shapes of increasing complexity.

2. 2.5D Propagation Model

2.1. Acoustic Wave Equations

Consider sound waves traveling through air confined by two curved surfaces, one being the mirror reflection of the other across the x/y plane of symmetry. These surfaces intersect on this plane, creating two distinct lines (i.e., a *contour*). Together, the surfaces and the contour delineate a wall, within which we can define an arbitrary finite control volume. Inside, a fluid particle of absolute density ρ_a is displaced by the incoming waves and moves at a velocity $\boldsymbol{v}$. Then, the change in the fluid mass within the control volume can be described as in [11],

$$\frac{\partial(\rho_a D)}{\partial t} = -\left[\frac{\partial(\rho_a D v_x)}{\partial x} + \frac{\partial(\rho_a D v_y)}{\partial y}\right], \qquad (1)$$

where $D(x, y)$ is a scalar parameter, which characterizes the slowly varying Euclidean distance along the z axis of the two

10.21437/Interspeech.2024-1749

surfaces enclosing the control volume (i.e., depth map) at coordinates x and y.

Considering mechanical attributes inherent to a vocal tract surface—inertia and elasticity—the enclosing wall displaces perpendicular to its surface as a direct consequence of the internally applied pressure. As we delineate the geometrical information of a wall surface using $D(x, y)$, the small displacement along the z axis can be approximated by a change in depth, i.e., $\Delta D = z(x, y, t)$. Hence, the final depth after the wall displacement at time t can be expressed as $D' = D + \Delta D$. Substituting the LHS and RHS of Equation 1 with D' and replacing the absolute density of the fluid particle as the sum of its static and dynamic parts (i.e., $\rho_a = \rho_0 + \rho$, where ρ_0 is the average atmospheric density and $\rho_0 \gg \rho$), one obtains,

$$D\frac{\partial \rho}{\partial t} + \rho_0 \frac{\partial z}{\partial t} = -\rho_0 \left[\frac{\partial (D v_x)}{\partial x} + \frac{\partial (D v_y)}{\partial y} \right]. \quad (2)$$

Here, the small terms of higher order are neglected (e.g., derivative of the product between ρ and z). $\partial z/\partial t$ denotes the rate of change of the vocal tract wall displacement along the z axis. Its value can be obtained by approximating the mechanical impedance of the vibrating wall (see the next subsection). As the change in air pressure and particle density inside the control volume is directly proportional to each other (i.e., $p = \rho c^2$), the above equation can be updated to obtain the continuity equation of the 2.5D wave solver as follows,

$$\frac{\partial p}{\partial t} = -\frac{\rho_0 c^2}{D} \left[\frac{\partial (D v_x)}{\partial x} + \frac{\partial (D v_y)}{\partial y} + \frac{\partial z}{\partial t} \right]. \quad (3)$$

The equation of motion for the 2.5D solver, derived from Newton's second law, does not explicitly depend on the depth of the control space. Hence, its form matches with the existing 2D wave solver [8, 6] and can be expressed as follows,

$$\beta \frac{\partial \boldsymbol{v}}{\partial t} + (1-\beta)\,\boldsymbol{v} = -\beta^2 \frac{\boldsymbol{\nabla} p}{\rho} + (1-\beta)\,\boldsymbol{v_b}, \quad (4)$$

where $\boldsymbol{v}(x, y, t)$ is the 2D vector that describes the velocity of the fluid particle and $\beta(x, y, t)$ is a scalar parameter that varies monotonically between 1 and 0, effectively transitioning between the momentum equation and boundary condition enforcement on the x/y mid-sagittal contour of the vocal tract wall (using some prescribed velocity $\boldsymbol{v} = \boldsymbol{v_b}$).

2.2. Wall Vibration Model

The control volume within a vocal tract can be treated as a resonance tube, allowing us to model the rate of change of the wall displacement $\partial z/\partial t$. Considering the elastic property of a vocal tract surface, the change in sound pressure induces both inward and outward movements of its walls. Consequently, such yielding walls exhibit a certain level of mechanical impedance that influences the acoustic wave transmission, particularly at lower frequencies [12]. The significance of this phenomenon in computational acoustics has been extensively examined in both theoretical studies [13] and practical applications [14, 5]. Hence, the proposed wave solver integrates a lumped-element mass-compliance-viscous loss system, which effectively aligns with the mechanical impedance characteristics of an acoustic tube surface.

Mathematically, the displacement of an infinitesimal surface element on a vocal tract side wall can be approximated using a spring-mass-damper system akin to the approach implemented by Kees and Ascher [5]. This formulation yields a second-order ODE describing the wall vibration,

$$W_c \cdot p = M \cdot \frac{\partial^2 z}{\partial t^2} + B \cdot \frac{\partial z}{\partial t} + K \cdot z, \quad (5)$$

where $M = M_0/\rho_0 c^2$, $B = B_0/\rho_0 c^2$ and $K = K_0/\rho_0 c^2$ are the mass, damping constant, and spring constant of the vocal tract wall per unit area, respectively. These parameters characterize the physical properties of an acoustic tube. W_c is the wall-coupling coefficient, which scales the exerted pressure on the vocal tract surface to control its oscillatory movement; it is necessary to account for the fact that, in the 2.5D model, wall displacement is restricted to the z axis only, keeping the contour stationary. As detailed in the next subsection, the solution of this ODE will employ the auxiliary variable $w = \partial z/\partial t$.

2.3. Discretized Wave Equations

We discretized the acoustic wave solver equations using first-order backward difference stencils in space and time on a staggered 2D grid, as in [8]. The acoustic parameters (p^n, v_x^n and v_y^n) and depth components ($\bar{D}$, D_x and D_y) of the solver are sampled across the entire domain at each time step. As described in our previous work [11], we computed tube depth by extracting the height of the tube surface along the z axis. This leads to the following discrete update rules of Equation 3 and 4, enhanced by the inclusion of a wall vibration parameter (w^n):

$$p^{n+1} = \frac{\bar{D} p^n - \rho_0 c^2 \Delta t\, (\widetilde{\boldsymbol{\nabla}} \cdot \boldsymbol{V}^n + w^n)}{\bar{D}}, \quad (6)$$

$$\boldsymbol{v}^{n+1} = \frac{\beta \boldsymbol{v}^{(n)} - \beta^2 \Delta t\, \widetilde{\nabla} p^{(n+1)}/\rho_0 + \Delta t(1-\beta)\boldsymbol{v_b}}{\beta + \Delta t(1-\beta)}, \quad (7)$$

where $\boldsymbol{V} = (\, D_x v_x,\ D_y v_y\,)$ and $\widetilde{\boldsymbol{\nabla}}$ denotes the standard discrete spatial derivative operator as in 2D FDTD. As proposed by Yokota et al. [15], the β parameter and locally reactive boundaries are used to model vocal tract wall absorption. This is done by setting $\beta = 0$ and $\boldsymbol{v_b} = \rho c\, \mu\, p_w \hat{\boldsymbol{n}}$, where p_w denotes the pressure sampled from the cell in front of the wall, $\hat{\boldsymbol{n}}$ is the unit normal vector directed towards the wall itself, and μ is the boundary admittance.

Due to a local pressure of zero at $t = 0$ (wall at rest), w^n is initialized to zero. Then, similarly to what was proposed in [5], we solve the discretized version of Equation 5 to obtain the wall displacement rate for the next time step,

$$w^{n+1} = \frac{M w^n + \Delta t (W_c \cdot p^{n+1} - K z^{n+1})}{M + B\Delta t}. \quad (8)$$

The pressure p^{n+1} is obtained from Equation 6, while the next displacement value derives from the following first-order backward difference,

$$z^{n+1} = w^n \Delta t + z^n. \quad (9)$$

In our 2D stencils, most quantities at each grid point are determined by current values, either sampled locally or from immediate neighbors. Only the computation of the velocity vector introduces additional dependencies across two neighboring pressure points computed at the next time step. However,

Figure 1: *Three vocal tract geometries for vowel /a/ having the same area functions but different cross-sectional shapes. We define the x axis along the length of the vocal tract.*

Allen and Raghuvanshi [8] demonstrated that this added computational complexity remains sufficiently low to allow for effective parallel processing implementations.

3. Experiments & Results

3.1. Model Validation

We validated the proposed 2.5D propagation model against a state-of-the-art 2D FDTD model [6] and a leading-edge 3D finite element (FE) [2] model for the following vowels: /a/, /i/, and /u/. For each vowel, we constructed straight 3D tubes of three distinct geometries and analyzed their acoustic output. These geometries, characterized by uniform length and area expansion but cross-sectional shapes of increasing complexity, were generated by simplifying the vocal tract's main conduit using its one-dimensional (1D) area functions [2].

Figure 1 shows the three vocal tract geometries, each characterized by a unique cross-sectional shape for the vowel /a/. These cross-sections have three different degrees of symmetry typically observed in actual vocal tracts [10]: a circle (full radial symmetry), an ellipse (symmetric along both y and z axis) and an irregular shape (symmetric along the z axis only). The acoustic properties of vocal tracts with circular cross-sections have been thoroughly studied using 1D [5], 2D [11, 6], and 3D [10, 1] models, making them a benchmark shape for assessing the newly proposed 2.5D model. However, they can only describe the emergence of fundamental modes. Conversely, vocal tracts with elliptical cross-sections break the radial symmetry of cylindrical geometry, allowing wave propagation in the transverse direction—perpendicular to the central axis. Until now, their acoustic characteristics have only been analyzed using 3D models [10, 1], positioning them as the subsequent validation step for the 2.5D model. We also examine the acoustic properties of an additional cross-sectional shape that is symmetric only across a single axis, generated by combining a circle and an ellipse, thereby increasing the geometrical complexity relative to the previous vocal tract shapes. By comparing the frequency responses of these vocal tract geometries, our objective was to gauge the extent to which the proposed 2.5D model could effectively produce perceptually relevant higher-order modes [16] that are absent in both 1D and 2D simulations.

Acoustic tubes resembling vocal tracts were built as 3D meshes for the FEM simulations. For the 2.5D simulations, a mid-sagittal contour (taken along the x/y plane) and a z axis depth map were extracted from each 3D tube and combined into 2.5D geometries. As thoroughly discussed by Arnela and Guasch [7], we represented vocal tracts by a flat contour, typically extracted from the mid-sagittal slice of a scaled 3D tube for the 2D FDTD simulations. The 2D approach is strictly limited to modeling cylindrical vocal tracts as it is unbounded along the z axis and cannot incorporate geometrical details of a tube across the sagittal plane. Nevertheless, we directly compared 2D results with the corresponding 2.5D and 3D simulations for the previously mentioned vocal tract geometries. This comparison underlines the limitations of the 2D model in synthesizing the acoustic features of tube geometries that have the same area functions but non-circular cross-sectional shapes.

For all three models, atmospheric density and speed of sound were assigned as follows: $\rho_0 = 1.14$ kg/m^3 and $c = 350$ m/s. For the 3D model, vocal tract walls were set to a standard boundary admittance $\mu = 0.005$ [11]. The 3D FE simulations were run with a mesh size of 2.5 mm and a time resolution of $\Delta t = 5 \times 10^{-6}$ s. We empirically adjusted the boundary admittance of the 2D ($\mu = 0.035$) and 2.5D ($\mu = 0.045$) models to match the 3D formants' bandwidths. The wall vibrations of the 2.5D vocal tract were modeled via standard values: $M_0 = 21$ kg/m^2, $B_0 = 8000$ kg/m^2 and $K_0 = 845000$ kg/m^{2}s^2 [5]. A 0.1 wall-coupling coefficient (W_c) yielded optimal results across all the geometries. The spatial resolution Δs of the 2.5D FDTD simulations was set to 0.75 mm. Compared to 2.5D, we set a higher spatial resolution of 0.28 mm for the 2D simulations to ensure their best performance [6]. The temporal resolution Δt of 2D and 2.5D models was restricted by the Courant-Friedrichs-Lewy condition, i.e., $\Delta t \leq \Delta s/\sqrt{2}c$. All models imposed Dirichlet boundary conditions at the mouth openings. The impulse response of each geometry was obtained by injecting a Gaussian pulse at the start of the vocal tract; the pressure variation was recorded at 3 mm inside the mouth opening for a total simulation time of 100 ms.

3.2. Results and Discussions

Figure 2 presents the 3D and 2.5D frequency responses obtained for different vocal tract geometries across all three vowels. For 2D simulations, the figure includes only the transfer functions of cylindrical vocal tracts. The 3D results (dashed lines) align with what is discussed in the vocal tract acoustics literature [5, 10]. Up until around 5 kHz, plane wave propagation can be assumed, and all three geometries display the same pattern of peaks (i.e., formants) and troughs for all vowels. Conversely, at higher frequencies, the effects of higher-order modes become visible. Formants' positions are not regularly spaced anymore, and additional resonances and antiresonances characterize each individual vocal tract geometry. Such acoustic features derive from the specific cross-sections and the associated modes of transverse propagation. The transfer functions derived from the 2D simulations (dotted lines) align with those of 3D vocal tracts featuring circular cross-sections, as the 2D approach can only model cylindrical tubes. For vocal tracts with elliptical or irregular cross-sectional shapes, the 2D model closely approximates 3D results within a specific frequency range where the planar wave assumption holds, highlighting the limitations in geometrical flexibility and accuracy of current 2D vocal tract models.

The 3D and 2.5D (solid lines) transfer function curves align closely up to about 12 kHz for all geometries, suggesting that the 2.5D model can reliably approximate the effects of non-circular vocal tract geometries (i.e., higher-order modes) with high perceptual significance. For instance, both models produce a significant dip around 10 kHz in their frequency responses

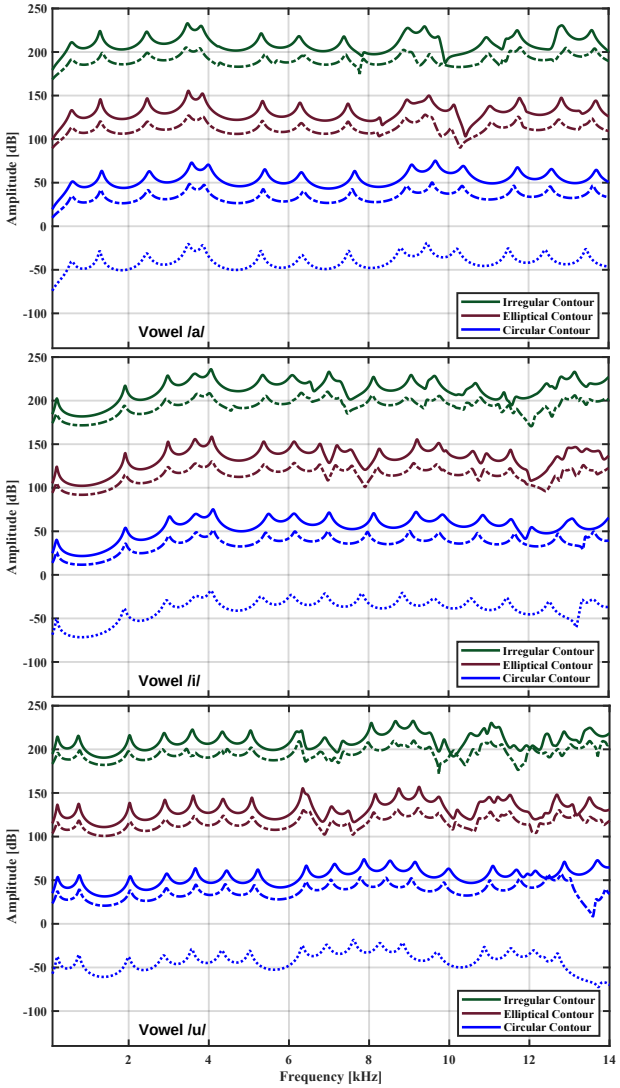

Figure 2: *Frequency responses (transfer functions) of the three vowels with different cross-sections, obtained with the 3D (dashed lines), 2.5D (solid lines) and 2D (dotted lines) models; curves were offset manually.*

of the elliptical vocal tract for the vowel /a/. Similar dips are also observed between 6 and 8 kHz in elliptical and irregular vocal tract geometries for vowels /i/ and /u/. Beyond 12 kHz, some discrepancies emerge, ranging from bandwidth mismatch at certain peaks to extra or missing troughs. Nonetheless, even at these higher frequencies, the general shape of the 2.5D curves remains akin to the benchmark 3D model.

To quantify the similarity between frequency responses, we measured the correlation between 2D and 3D curves, as well as between 2.5D and 3D curves. This analysis evaluates the extent to which 2D and 2.5D simulations can precisely approximate the higher spectral features in their transfer functions as produced by 3D models across various vocal tract geometries. For the 2D solver, the correlation was determined by directly comparing its frequency response with that of 3D tubes for all three geometries. Figure 3 presents the cumulative Pearson correlation coefficient for the vowel /u/. As anticipated, the transfer function of the 2D model (dotted lines) exhibits a statistical resemblance to that of a 3D tube with circular cross-sections. This

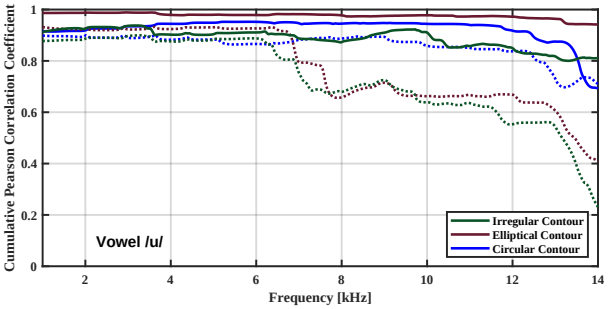

Figure 3: *Cumulative Pearson correlation coefficient between 2D-3D (dotted lines) and 2.5D-3D (solid lines) transfer function curves for the vowel /u/.*

similarity is evident as the correlation coefficient remains above 0.8 up to 13 kHz. For vocal tract geometries with non-circular cross-sectional shapes, the correlation coefficient significantly drops at about 7 kHz. Beyond 10 kHz, the 2D and 3D transfer functions do not match as they drop below 0.7, demonstrating the 2D model's limitations in accurately reproducing the effects of higher-order modes. In contrast, the transfer functions of the 2.5D model (solid lines) for all three geometries exhibit a high degree of similarity with the corresponding 3D outputs, with correlation coefficients surpassing 0.8 even at higher frequencies. While we solely focused on the transfer functions of the vowel /u/ in this discussion, owing to its geometrical complexity, similar results were also noted for other vowels.

All simulations were conducted on a CPU workstation powered by an Intel Core i7-8750H processor. A comparative analysis was carried out to measure the computational performance of the 2.5D model. For vowel /u/, the 3D model took 0.5 hours for all tube geometries. Meanwhile, the performance of the 2D and 2.5D FDTD models solely depends on the size of the computational grid, which is determined by the spatial resolution of simulations. Due to an extremely high spatial resolution requirement [17], the 2D model took approximately 0.75 hours for all three geometries, and they were accommodated within the same 770×119 grid. In contrast, the 2.5D model took 120 s, and accommodated all three tubes in a grid size of 290×53. Notably, even against the fastest 3D and 2D simulations, the 2.5D model achieved a speed-up factor close to an order of magnitude. This efficiency is particularly impressive considering the 3D model utilized the C++ FEniCSx platform (`http://fenicsproject.org/`), whereas the 2.5D model was developed in MATLAB without specialized optimization. Theoretically, our proposed model can achieve real-time performance through GPU implementation [17].

4. Conclusion

We introduced a 2.5D wave propagation model that simulates acoustics in irregularly shaped vocal tract geometries. Although restricted to mid-sagittal symmetry, our model surpasses traditional 1D and 2D models that are confined to circular cross-sections. The underlying FDTD wave solver reliably approximates higher-order spectral features similar to 3D and offers computational efficiency similar to a lightweight 2D solution. Compared to full 3D models, this results in significantly reduced computational scaling as the domain size increases. Our next step is to incorporate vocal tract side branches and develop a graphics card-accelerated version of the 2.5D wave solver to demonstrate a real-time articulatory speech synthesizer.

5. Acknowledgement

This work is supported by the Natural Sciences and Engineering Research Council (NSERC) of Canada and the Canadian Institutes for Health Research (CIHR).

6. References

[1] D. R. Mohapatra, M. Fleischer, V. Zappi, P. Birkholz, and S. Fels, "Three-dimensional finite-difference time-domain acoustic analysis of simplified vocal tract shapes," *Proc. Interspeech 2022*, pp. 764–768, 2022.

[2] P. Birkholz, S. Kürbis, S. Stone, P. Häsner, R. Blandin, and M. Fleischer, "Printable 3d vocal tract shapes from mri data and their acoustic and aerodynamic properties," *Scientific data*, vol. 7, no. 1, p. 255, 2020.

[3] H. Takemoto, P. Mokhtari, and T. Kitamura, "Acoustic analysis of the vocal tract during vowel production by finite-difference time-domain method," *the Journal of the acoustical society of America*, vol. 128, no. 6, pp. 3724–3738, 2010.

[4] R. Blandin, M. Arnela, R. Laboissière, X. Pelorson, O. Guasch, A. V. Hirtum, and X. Laval, "Effects of higher order propagation modes in vocal tract like geometries," *The Journal of the Acoustical Society of America*, vol. 137, no. 2, pp. 832–843, 2015.

[5] K. van den Doel and U. M. Ascher, "Real-time numerical solution of webster's equation on a nonuniform grid," *IEEE transactions on audio, speech, and language processing*, vol. 16, no. 6, pp. 1163–1172, 2008.

[6] V. Zappi, A. Vasuvedan, A. Allen, N. Raghuvanshi, and S. Fels, "Towards real-time two-dimensional wave propagation for articulatory speech synthesis," in *Proceedings of Meetings on Acoustics 171ASA*, vol. 26. Acoustical Society of America, 2016, p. 045005.

[7] M. Arnela and O. Guasch, "Two-dimensional vocal tracts with three-dimensional behavior in the numerical generation of vowels," *The Journal of the Acoustical Society of America*, vol. 135, no. 1, pp. 369–379, 2014.

[8] A. Allen and N. Raghuvanshi, "Aerophones in flatland: Interactive wave simulation of wind instruments," *ACM Transactions on Graphics (TOG)*, vol. 34, no. 4, pp. 1–11, 2015.

[9] S. Bilbao, A. Torin, and V. Chatziioannou, "Numerical modeling of collisions in musical instruments," *Acta Acustica united with Acustica*, vol. 101, no. 1, pp. 155–173, 2015.

[10] M. Arnela, S. Dabbaghchian, R. Blandin, O. Guasch, O. Engwall, A. Van Hirtum, and X. Pelorson, "Influence of vocal tract geometry simplifications on the numerical simulation of vowel sounds," *The Journal of the Acoustical Society of America*, vol. 140, no. 3, pp. 1707–1718, 2016.

[11] D. R. Mohapatra, V. Zappi, and S. Fels, "An extended two-dimensional vocal tract model for fast acoustic simulation of single-axis symmetric three-dimensional tubes," *Proc. Interspeech 2019*, pp. 3760–3764, 2019.

[12] K. Ishizaka, J. French, and J. Flanagan, "Direct determination of vocal tract wall impedance," *IEEE Transactions on Acoustics, Speech, and Signal Processing*, vol. 23, no. 4, pp. 370–373, 1975.

[13] E. Kerschen and J. Johnston, "Mode selective transfer of energy from sound propagating inside circular pipes to pipe wall vibration," *The Journal of the Acoustical Society of America*, vol. 67, no. 6, pp. 1931–1934, 1980.

[14] W. Kausel, D. W. Zietlow, and T. R. Moore, "Influence of wall vibrations on the sound of brass wind instruments," *The Journal of the Acoustical Society of America*, vol. 128, no. 5, pp. 3161–3174, 2010.

[15] T. Yokota, S. Sakamoto, and H. Tachibana, "Visualization of sound propagation and scattering in rooms," *Acoustical science and technology*, vol. 23, no. 1, pp. 40–46, 2002.

[16] B. B. Monson, E. J. Hunter, A. J. Lotto, and B. H. Story, "The perceptual significance of high-frequency energy in the human voice," *Frontiers in psychology*, vol. 5, p. 587, 2014.

[17] V. Zappi, A. Allen, and S. S. Fels, "Shader-based physical modelling for the design of massive digital musical instruments." in *NIME*, 2017, pp. 145–150.